ISSN 1063-7729, Astronomy Reports, 2019, Vol. 63, No. 8, pp. 666–686. © Pleiades Publishing, Ltd., 2019.
Russian Text © The Author(s), 2019, published in Astronomicheskii Zhurnal, 2019, Vol. 96, No. 8, pp. 653–673.

Characteristic Features of the Colors of Shower Meteors and Sporadic Meteors from Observations with the Mini-MegaTORTORA System

V. S. Usanin[1]*, Yu. A. Nefedyev[1], and M. G. Sokolova[1]*****

[1] *Kazan (Volga Region) Federal University, Kazan, 420008 Russia*

Received December 24, 2018; revised March 20, 2019; accepted March 22, 2019

Abstract—Results of BVR observations of meteors in the Perseid, Taurid, Orionid, Geminid, and Lyrid showers, as well as sporadic meteors, carried out with the Mini-MegaTORTORA system are presented. Two-color diagrams for the brightness maxima are constructed. It is shown that meteors in the Perseid, Taurid, and Geminid showers form clusters in the two-color diagrams. Variations in color with a temporal resolution of 0.1 s are considered for some meteors.

DOI: 10.1134/S1063772919080055

1. INTRODUCTION

Meteor astronomy is one of the few areas of science in which visual observations still have importance to this day. One of the important characteristics derived in observations of meteors is their color [1]. Detailed descriptions of the colors of meteors are present in European, Chinese, and Japanese historical chronicles starting from the 11th century [2, 3]. Statistical studies of the visual colors of sporadic and shower meteors have been carried out [4, 5]. Together with the colors characteristic for thermal blackbody radiation and the colors of normal stars, such as blue, white, yellow, orange, and red, meteors sometimes also display green, pink, and violet colors [5–7].

At the same time, the perception of colors by the human eye is very subjective, especially when the illumination is weak. Known instrumental and semi-instrumental methods from astrophysics are applied in meteor astronomy to the extent this is possible.

In [8, 9], the color index of a meteor was taken to be the difference between its photographic and visual magnitudes at the brightness maximum. A dependence between the color index and magntiude was detected, without any dependence on velocity. It has been suggested that this could be due to the physiological Purkinje effect—the shift of the spectral sensitivity for human sight with the brightness of an observed source. To test this hypothesis, photoelectric observations with blue and green, and also with green and red, filters were carried out simultaneously with photographic and visual observations [10, 11]. It turned out that the Purkinje effect can only partially explain the magnitude dependence of the color indices of meteors. Most subsequent multi-color photometry of meteors has confirmed these conclusions.

A statistical method was used to find the magnitude dependences of the color indices of meteors found on photographic plates of the Palomar atlas obtained with blue-sensitive emulsion and with a red filter [12]. Color indices of meteors have been determined using visual observations of meteors with binocular telescopes simultaneously with no filter and with blue and red filters [13], and also using visual [14] and photographic [15] observations obtained simultaneously with no filter and with blue, yellow, orange, and red filters. Qualitatively the same magnitude dependence for the color indices was found for points on meteor trails away from the maximum brightness, but with different numerical parameters [16]. Differences between photometric systems used in various studies of meteor color indices have been discussed in the literature [17]. Visual color estimates were used with a statistical method to determine the color indices for meteors with various magnitudes in various showers [18]. Narrow-band color indices have been considered as an alternative to spectroscopic observations of meteors [19]. A velocity dependence for meteor color indices was detected only in [20], with this dependence being much weaker than the magnitude dependence.

Spectroscopic observations of meteors have an even longer history than multi-color photometry. Meteor spectra consist of a relatively weak continuum together with atomic emission lines and molecular

*E-mail: Vladimir.Usanin@kpfu.ru
**E-mail: star1955@mail.ru
***E-mail: smarina.63@mail.ru

bands. The traditional standard classification is based on the character of a spectrum at maximum brightness, and also incorporates informaton about the strongest features detected. This system has four main types of spectra: Y—the H and K lines of Ca II are the strongest features in the blue–violet; X—either the D-lines of Na I, or the lines near 5180 Å or 3835 Å of Mg I, give the strongest feature in either the orange–green or the blue–violet; Z—the lines of Fe I, or those of Cr I, give the strongest feature in either the orange–green or blue–violet; W—peculiar spectra [21, 22]. It was later elucidated that meteor spectra have two components: a main component with a temperature of about 4000 K and a secondary component with a temperature of about 10 000 K. The standard classification reflects the variable intensity of the high-temperature part, which forms from 0.02 to 5% of the vapor envelopes of meteors [23]. Video spectra of meteors have low resolution, and usually only Mg, Na, and Fe lines can be resolved. Therefore, another classification based on the positions of the intensities of these lines on a ternary Na–Mg–Fe diagram is also used, enabling the identification of the following classes: normal, Na-poor, Fe-poor, Enhanced-Na, Irons, Na-free, and Na-rich. The majority of meteoroids fall into one of the first four of these classes [24].

An absence of a correlation between the visual colors of meteors and their spectral type was noted in [25]. Meteors with different types of spectra can belong to the same shower. A correlation between the velocity of a meteor and the degree of excitation of its atoms (i.e., the relative intensities of different emission lines) was found [21]. These results obtained in earlier studies, in general terms, are still valid today [26, 27]. However, it remains unclear whether spectroscopic observations can provide information about the nature of meteors [28].

The use of non-standard photometric systems in many studies hinders the ability to reproduce and compare different results. In particular, it is not possible to drawn conclusions about the mean color indices of meteor showers based on earlier observations. For example, it follows from [15] that the mean color indices grow by more than 1.5^m in the sequence Taurids–Orionids–Perseids, whereas a similar growth occurs in the sequence Geminids–Perseids–Taurids–Orionids according to [18], and the mean color indices of these four showers differ by only 0.1^m according to [20]. The contradiction between the presence of a dependence of the intensities of spectral emission lines on the meteor velocity but an absence of such a dependence for the color indices has also been discussed [14, 20].

Thus, the development of instrumental methods for studying meteor colors that would enable comparisons with visual data, and would be free of subjectivity and easily reproducible, remains topical.

2. TWO-COLOR DIAGRAM METHOD

Two-color diagrams are well known in astrophysics as a means of analyzing color excesses. From the very start of multi-color photometry, they have been used to describe the intrinsic radiation of stars [29]. Two-color diagrams also lie at the basis of the spectral classification of asteroids through an analysis of their reflected light [30]. The same method is widely applied to objects in the outer solar system [31–33]. Two-color diagrams have also been constructed for artificial Earth satellites [34].

A line corresponding to the thermal radiation of perfect blackbodies with various temperatures can be drawn on two-color diagrams. The sequence of normal stars on diagrams constructed for the visible range is located not far from this line, since only a small fraction of the radiation is absorbed in lines in this spectral range, and the absorption lines are distributed fairly evenly in wavelength. If an astrophysical object deviates strongly from these sequences, this immediately identifies it as unusual.

We should especially mention the $B-V$ vs. $V-R$ diagram constructed for a wide range of applications in astrophysics, since the transmission bands for all three of these filters lie in the visible range. These filters are close to, but not identical to, the RGB filters of the Bayer system used in consumer electronics to obtain and reproduce information about visual colors [35]. In essence, the RGB system copies the principle behind human cone vision. Consequently, the BVR system is standard in astrophysics, and can be used to obtain information about the colors that are perceived by a human observer.

3. OBSERVATIONAL MATERIAL

The observations for which results are presented in this paper were carried out at our request using the Mini-MegaTORTORA (MMT-9) multi-channel monitoring telescope of the Kazan Federal University, located at the site of the Special Astrophysical Observatory of the Russian Academy of Sciences [36]. This system has nine cameras installed in pairs on five equatorial mounts. The main elements of each camera are a Canon EF85/1.2 lens, an Andor Neo sCMOS sensor, and a coelostat mirror. The temporal resolution of MMT-9 is 0.1 s. BVR filters in the Johnson–Cousins system can be introduced into the light path of each camera, as needed [37]. The channels operating with B filters have the lowest

sensitivity, and those operating with the R filters the highest sensitivity.

A detailed description of the MMT-9 photometric system is given in [38]. The MMT-9 software estimates the intensity along a meteor trail extracted using a Hough transform [39]. Both the integrated (i.e., calculated from the intensity integrated along the meteor trail) brightnesses in individual frames [40] and the intensity profile along a meteor trail are entered into a database. Note that, in [8, 9, 11], where photographic emulsion was used as a light detector, the frames were taken with a slow shutter speed; therefore, the actual exposure time for a meteor was much shorter than the exposure times for the comparison stars, and deriving the magnitude of a meteor required a correction for the velocity. This does not pose difficulties, since the apparent velocities of stars are determined by the known angular rotational velocty of the Earth, and the apparent velocity of the meteor can be measured using a rotating shutter [41, 42]. It is obvious that the correction for the velocity does not depend on the photometric band used, and so cancels out when a difference of magnitudes of the same meteor obtained with the same lenses and detectors, but different filters, is taken; i.e., it is not present in the color indices [15, 16]. Modern detectors are able to take frames with shutter speeds that are shorter than the duration of a meteor event, so that the exposure time for stars in a single frame becomes equal to the exposure time for the meteor trail, and no correction for the velocity is needed to determine the magnitudes [43], all the moreso for determining color indices. We used the integrated magnitudes of meteors in individual frames accessible in the MMT-9 database.

The BVR observations of meteors were obtained primarily during the major meteor showers from May 2015 through April 2016. As for other observations of meteors carried out with MMT-9, preliminary results were automatically entered into the database[1] . During these observations, the channels were synchronized in time. Lack of synchronization between the time stamps in the database does not indicate that the channels are physically out of synch, as is demonstrated by an analysis of astrometric data. In our current study, we considered meteors observed in all three filters when the maximum V brightness was observed. Observations in which the color indices could potentially be determined incorrectly due to the registration of different parts of the meteor track in different filters were excluded from our analysis. First and foremost, this corresponds to cases when the image of a meteor crosses a frame boundary. In addition, the MMT-9 software automatically measures only one continuous part of a trail, making it necessary to note cases when the image of a meteor trail is intermittent (separation of a persistent train in the meteor wake; a weak meteor observed at the sensitivity limit). Table 1 presents a list of identifiers for 66 meteors in the MMT-9 database that were included in our sample.

Based on the principles considered in [44], we verified the membership of the meteors in the major showers: η-Aquariids, Southern δ-Aquariids, Perseids, Draconids, Southern Taurids, Orionids, Northern Taurids, Leonids, Geminids, Ursids, Quadrantids, Lyrids. As a result, eight meteors were identified as Perseids, six as Southern Taurids, one as an Orionid, two as Northern Taurids, 15 as Geminids, and one as a Lyrid; the remaining 33 were not identified with any of these showers. The identification results for individual meteors are also given in Table 1.

4. BRIEF INFORMATION ABOUT THE STUDIED SHOWERS

Based on general considerations, we expect the color of a meteor to depend to some extent on its velocity and the chemical composition of the meteoroid from which it arose. The velocity of a meteoroid depends directly on the orbital elements of its parent body (comet or asteroid). The chemical composition could also be related indirectly to the orbital elements: the loss of volatile matter from a small body depends on the intensity and frequency of heating of the body when it approaches the Sun. Therefore, comets (small bodies that emit a large amount of volatile matter) and asteroids (small bodies that emit almost no volatile matter) are usually found in appreciably different orbits. We will now present some brief information about the meteor showers we have identified in the BVR MMT-9 observations and their origins [45, 46].

The parent body of the Perseids (PER) is Comet 109P/Swift–Tuttle. Its perihelion distance is $q = 0.96$ AU, aphelion distance is $Q = 51$ AU, period of revolution around the Sun is $P = 133$ yrs, and the inclination of its orbit to the plane of the ecliptic is $i = 113°$. Thus, this is a Halley-type comet. The mean velocity with which the meteoric bodies enter the Earth's atmosphere is 60.1 km/s.

The Southern (STA) and Northern (NTA) Taurids are a branch of the large Taurid complex (TAU), whose main body is Comet 2P/Encke. The orbital elements of this comet are $q = 0.34$ AU, $Q = 4.1$ AU, $P = 3.3$ yrs, $i = 11.8°$. It differs from the Jupiter-family comets in its smaller aphelion distance, and it is currently classified as an Encke-type comet. A large number of asteroids were also discovered in this

[1] http://www.astroguard.ru/meteors

Table 1. List of studied meteors

No.	Id B	Id V	Id R	Shower	No.	Id B	Id V	Id R	Shower
1	7616498	7616500	7616501		34	9167226	9167228	9167227	ORI
2	8292831	8292834	8292832		35	9178196	9178199	9178197	
3	8293684	8293686	8293685		36	9187883	9187884	9187885	NTA
4	8316513	8316514	8316512		37	9187922	9187923	9187924	
5	8339660	8339663	8339661		38	9188079	9188080	9188081	STA
6	8344020	8344018	8344019		39	9188119	9188121	9188123	
7	8356932	8356934	8356933		40	9442888	9442890	9442891	NTA
8	8358097	8358101	8358100	PER	41	9477959	9477957	9477960	STA
9	8358347	8358349	8358348		42	9523610	9523609	9523611	
10	8359289	8359291	8359290	PER	43	9697469	9697471	9697470	GEM
11	8363316	8363318	8363317		44	9697483	9697482	9697484	GEM
12	8365630	8365632	8365629		45	9698051	9698052	9698053	GEM
13	8369150	8369151	8369152		46	9701729	9701733	9701732	GEM
14	8370806	8370808	8370810		47	9701813	9701814	9701815	
15	8370871	8370873	8370872	PER	48	9702155	9702156	9702157	GEM
16	8371360	8371362	8371363		49	9705210	9705211	9705212	GEM
17	8372337	8372340	8372338	PER	50	9705823	9705824	9705825	GEM
18	8373345	8373347	8373346	PER	51	9705858	9705859	9705860	GEM
19	8378202	8378203	8378204	PER	52	9705863	9705865	9705864	
20	8378429	8378430	8378427	PER	53	9706791	9706792	9706793	GEM
21	8388492	8388493	8388494		54	9706850	9706852	9706854	GEM
22	8396589	8396590	8396591		55	9706975	9706977	9706976	
23	8397092	8397094	8397093	PER	56	9709172	9709175	9709174	GEM
24	8403654	8403656	8403655		57	9710964	9710965	9710967	GEM
25	9032882	9032884	9032883		58	9711658	9711659	9711660	GEM
26	9034032	9034034	9034033		59	9720197	9720201	9720200	GEM
27	9041258	9041260	9041259		60	9720350	9720353	9720355	
28	9050887	9050888	9050889	STA	61	9722168	9722169	9722170	GEM
29	9051567	9051568	9051569		62	9804765	9804766	9804764	
30	9053143	9053145	9053146	STA	63	10025040	10025039	10025041	
31	9055178	9055182	9055179	STA	64	10054057	10054060	10054062	
32	9165236	9165238	9165237		65	10397610	10397613	10397614	
33	9165926	9165928	9165927	STA	66	10397723	10397725	10397726	LYR

complex [47]. The mean velocity of these meteors is 28.8 km/s for STA and 30.1 km/s for NTA.

The Orionids (ORI) are one of two showers (together with the η-Aquariids) formed by Comet 1P/Halley. This is the prototype of Halley-type comets: $q = 0.59$ AU, $Q = 35$ AU, $P = 75$ yrs, $i = 162°$. According to an old classification, it is part of the Neptune family. The mean velocity of entry into the Earth's atmosphere is 67.2 km/s.

The parent body of the Geminids (GEM) is believed to be the asteroid Phaethon (3200). The orbit of this asteroid has the elements $q = 0.140$ AU, $Q = 2.4$ AU, $P = 1.43$ yrs, and $i = 22°$, suggesting it belongs to the Apollos. Signs of cometary activity were observed during one of the perihelion passages of this asteroid [48], however, its aphelion distance is much smaller than those of comets that manifest activity in each apparition. The structure of this shower suggests a cometary model for its formation [49]. These meteors have a mean velocity of 35.6 km/s.

Lyrids (LYR) are associated with the long-period Comet Thatcher (C/1861 G1), which has been observed during only one return to the Sun in 1861 and has the orbital elements: $q = 0.92$ AU, $Q \approx 110$ AU, $P \approx 415$ yrs, $i = 80°$. The mean velocity of these meteors is 48.0 km/s.

We will refer to meteors that were not identified with the above showers as sporadic meteors (SPO).

5. TWO-COLOR DIAGRAM FOR BRIGHTNESS MAXIMA

Figure 1 presents the two-color diagram for the brightness maxima in the V filter for all 66 meteors considered. To help with orientation, the line corresponding to thermal radiation of perfect blackbodies of various temperatures [50] and the main sequence [37] are shown. The background of the diagram was constructed by comparing the BVR colors with the corresponding RGB colors without corrections for the transformation between the photometric systems [35] (these corrections have meaning if the spectrum of an observed source is known at least approximately), white color corresponds to the Sun [51], and the gamma correction (which determines the semitoning) was taken to be equal to the standard value of 2.2. Note that the boundaries of the region in the two-color diagram occupied by all the meteors could be determined by observational selection effects.

As Fig. 1 shows, meteors of the Perseid, Taurid, and Geminid showers form clusters in the two-color diagram, in accordance with their membership in these showers, while the sporadic meteors are scattered throughout the diagram. The color indices of the mean point of the Perseid group are $\overline{B-V} = +0.76^m$ and $\overline{V-R} = +1.02^m$, the rms distance of the meteors from the mean point on the diagram is $\sigma = 0.22^m$, and the largest distance from the mean point is 0.34^m. The mean point for the Taurid group is $\overline{B-V} = +0.68^m$, $\overline{V-R} = +0.44^m$; the rms distance of the meteors from the mean point is $\sigma = 0.10^m$; and the largest distance from the mean point is 0.15^m. The mean point of the Geminid group is $\overline{B-V} = +0.53^m$, $\overline{V-R} = +0.49^m$; the rms distance of the meteors from the mean point is $\sigma = 0.21^m$; and the largest distance from the mean point is 0.30^m. The distance between the mean points for the Perseids and Taurids is 0.58^m, between the Perseids and Geminids is 0.57^m, and between the Taurids and Geminids is 0.16^m (Fig. 2). Since the distance between the mean points for the Perseids and Taurids is larger than the sum of their radii, these two groups are fully separate from each other. Also, since the distances between the mean points for the rest two pairs of groups are larger than the individual radii of some groups of these pairs, the mean point for the Geminid group lies beyond the Taurid group and the mean points for the Perseid and Geminid groups are each beyond the other group. Other factors, such as the individual characteristics of the meteors, including their magnitudes, and uncertainties, including uncertainty in the determination of the brightness maximum, did not lead to scatter of the clusters formed by the showers.

Both the Northern and Southern Taurids are located closest to the line for a perfect blackbody, in white color, which corresponds to a temperature of 5000–6000 K and stellar spectral type G. The Geminids partially overlap with the Taurids, and are also located in the directions of violet and orange colors. The Perseids and one Orionid are located in the right part of the diagram, between the pink and orange colors. Note that another meteor in the Orionid shower (identifiers in the MMT-9 database 9188219, 9188222, 9188220) was not included in the final sample, since it was not clear whether it had reached its maximum brightness before the separation of the persistent train. The color indices calculated from the last frames before the separation could also place it amongst the Perseid group. The only meteor from the Lyrid shower that was observed in three filters ended up in the left part of the diagram, in the region of blue colors, although other Lyrids that were not observed in the B filter, and therefore did not make it into our sample, do not have negative $V-R$ values.

It is usually supposed that the temperature of a meteor grows with its velocity; since hundreds of lines are emitted simultaneously in a meteor, we would expect the appearance of some sort of Wien's displacement law, with the color index decreasing with

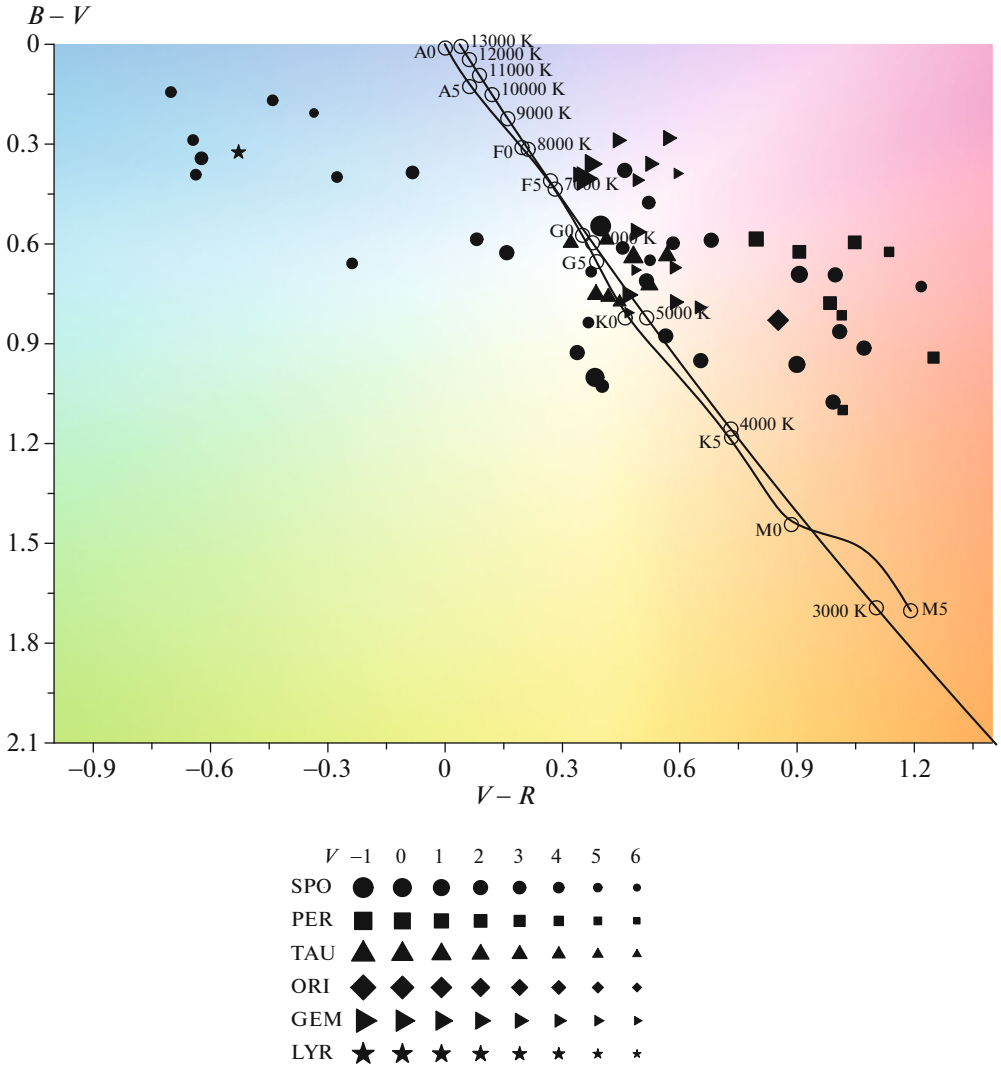

Fig. 1. Two-color diagram for the brightness maxima.

increasing velocity. However, the earlier observations indicated the opposite tendency [20], and we can see the same result in Fig. 1: meteors of the high-velocity Perseid and Orionid showers are much redder than those of the lower-velocity Geminid and Taurid showers. A meteor of the Lyrid shower with an intermediate velocity is located on the opposite side of the diagram from the high-velocity showers, and not between the high-velocity and low-velocity showers.

The Taurids are close to the Geminids in the diagram, and both these showers could have a mixed comet–asteroid origin [47, 49].

The differences of the locations of the shower meteors in the two-color diagram from their locations in the Na–Mg–Fe ternary spectral diagram are appreciable [27]. For example, meteors of the Lyrid shower are located on the opposite side from the Perseids and Orionids in the two-color diagram, but these three showers are located in the same region of the Na–Mg–Fe diagram. At the same time, the Taurids and Geminids are located in the same region in the two-color diagram, but in opposite regions of the Na–Mg–Fe diagram. Thus, the color classification of meteors does not agree with their spectral classification in these cases, and contains other information that requires additional study.

6. TWO-COLOR DIAGRAMS FOR INDIVIDUAL METEORS

The high temporal resolution of the MMT-9 makes it possible to trace variations of the colors of a meteor in time steps of 0.1 s. Figures 3–26 present tracks on two-color diagrams of meteors whose color indices were determined over the entire time from their appearance to their disappearance, with no intersections with frame boundaries, according to the

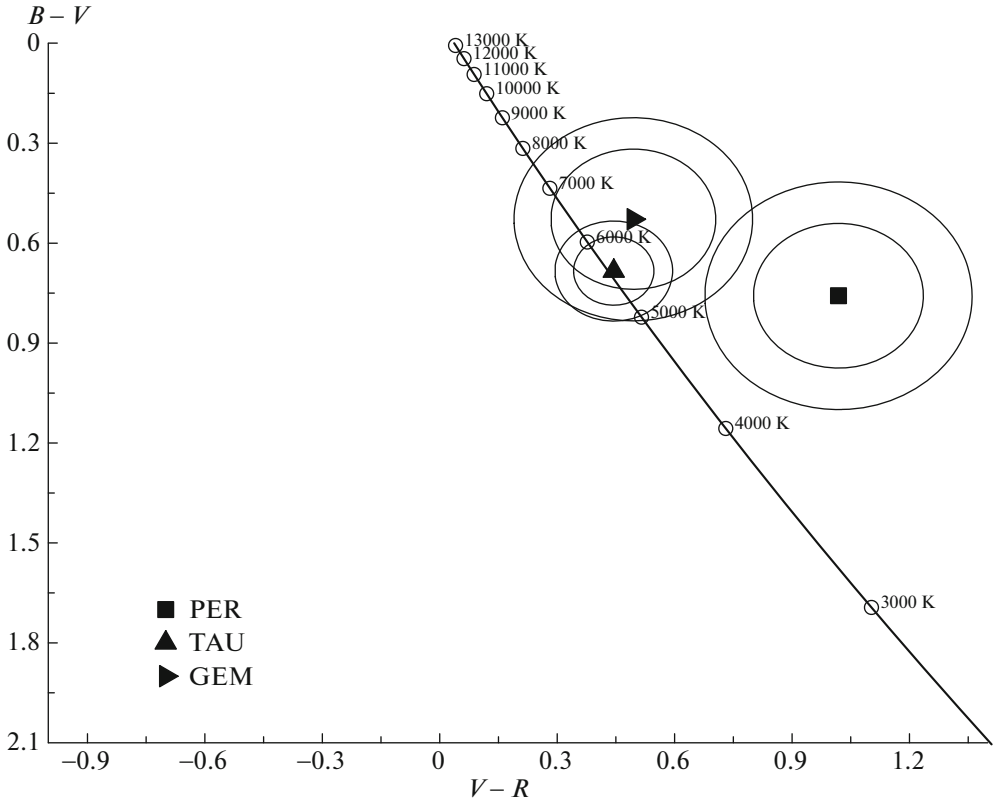

Fig. 2. Two-color diagram for the Perseid, Taurid, and Geminid showers. The mean points of the groups, rms distances of the meteors from the mean points, and the largest distances from the mean points are shown.

least sensitive channel and based on no fewer than four successive frames. The order of the figures is: sporadic meteors (Figs. 3–12), Perseids (Fig. 13), Taurids (Figs. 14–16), Geminids (Figs. 17–25), Lyrids (Fig. 26); within each group, the figures are sorted in ascending order of $V - R$, i.e., from left to right in the diagram. The chronological sequence of frames is denoted by the numbers around the points in each figure.

Let us first consider the diagrams for the shower meteors.

Note the move of the meteor of the Perseid shower (Fig. 13) from the upper right to the lower left in the diagram, in the direction of green colors. The same tendency for $B - V$ to grow as $V - R$ decreases is inherent to other observed meteors in this shower, which didn't satisfy some criteria for constructing these diagrams. An inspection of the images of meteors in the MMT-9 databases showed that the Perseids are characterized primarily by the formation of persistent trains that are brighter in the V filter than in B and R; i.e., that have green colors. It is known that this represents emission of the auroral line of neutral atomic oxygen with wavelength 5577 Å [52].

None of the observed meteors of the Geminid shower (Figs. 17–25) had self-intersecting tracks on the two-color diagrams, while such self-intersections are present for the Taurids (Figs. 14–16).

The tracks for sporadic meteors on the two-color diagrams (Figs. 3–12) have very diverse forms. We can find analogs for meteors No. 6 (Fig. 10) and No. 3 (Fig. 11) amongst the Geminids—Nos. 49, 43, 50 (Figs. 17, 22, 23) and No. 58 (Fig. 25), respectively—but these were both observed in August, which rules out membership in the Geminids, which are active only in December.

Given that the number of observed meteors in each group is modest, these conclusions must be considered tentatively for the moment.

7. CONCLUSION

The BVR observations carried out at our request with the Mini-MegaTORTORA system and the application of two-color diagrams leads to the conclusion that the main factor determining the colors of observed meteors in the Perseid, Taurid, and Geminid showers in the visible is their membership in a given shower. The magnitude dependence of the colors and measurement uncertainty, including uncertainty in determining the brightness maximum, did not act to scatter the clusters formed by the showers in the

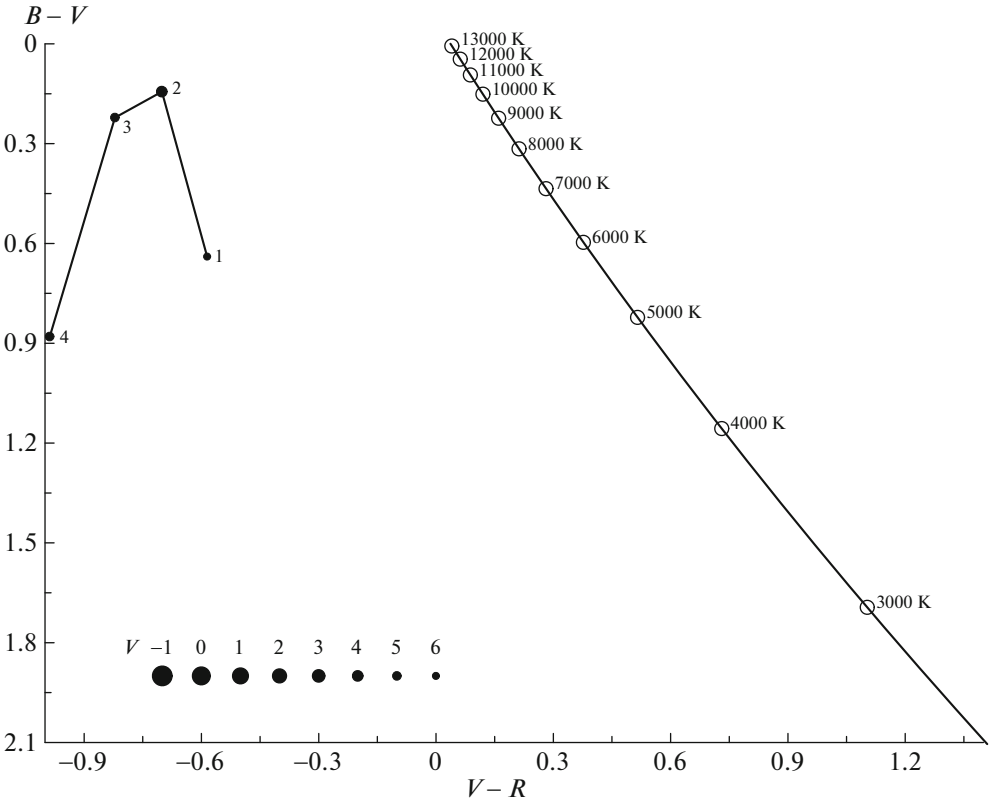

Fig. 3. Two-color diagram for meteor No. 52 (SPO).

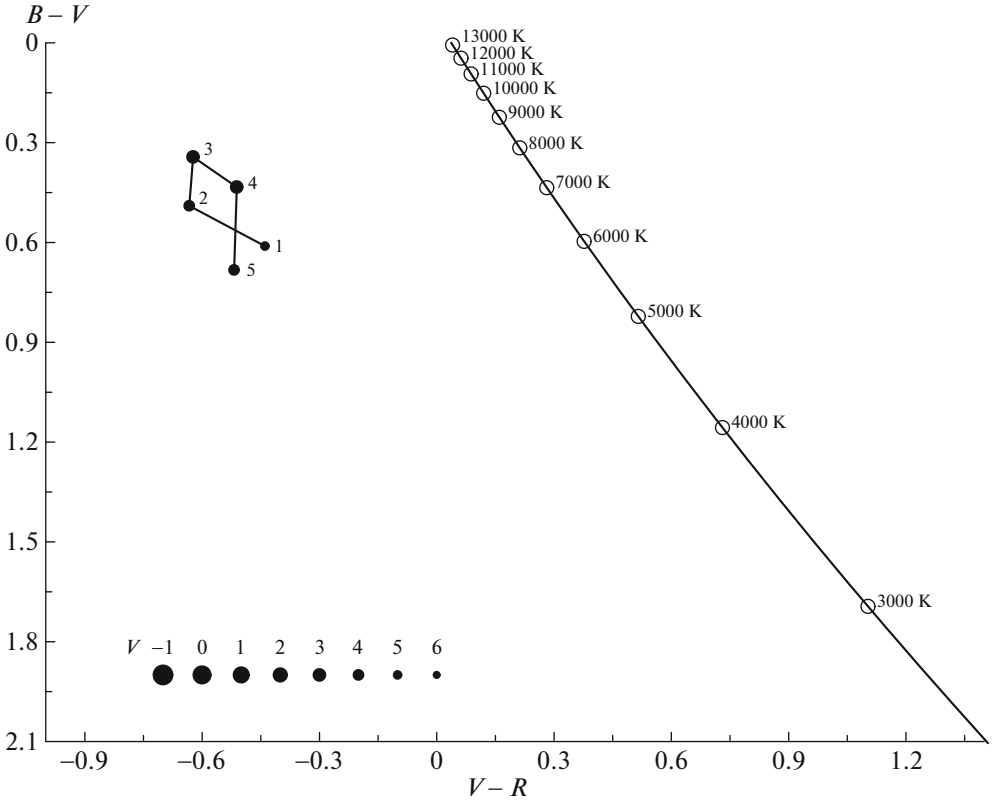

Fig. 4. Two-color diagram for meteor No. 55 (SPO).

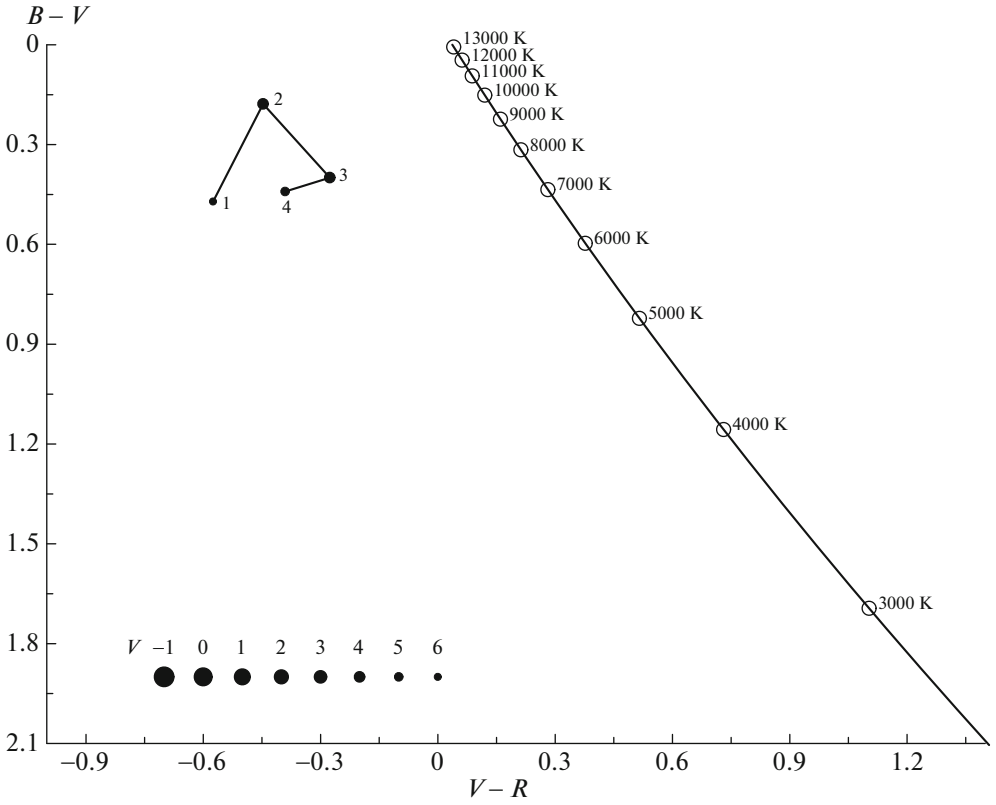

Fig. 5. Two-color diagram for meteor No. 25 (SPO).

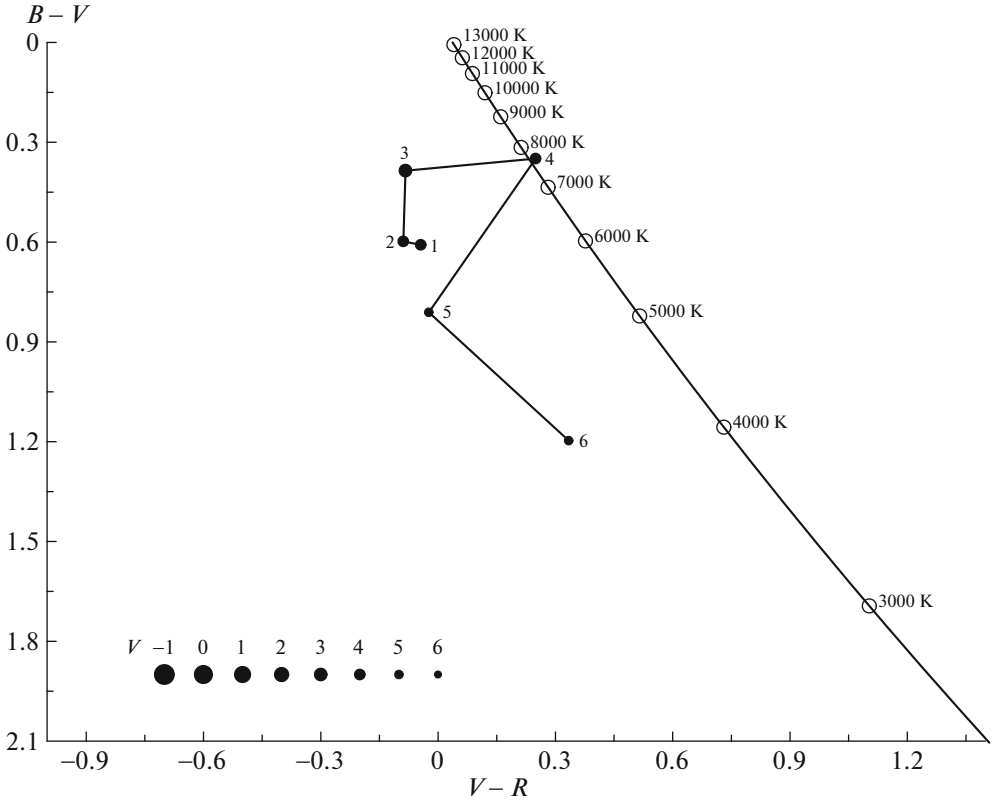

Fig. 6. Two-color diagram for meteor No. 65 (SPO).

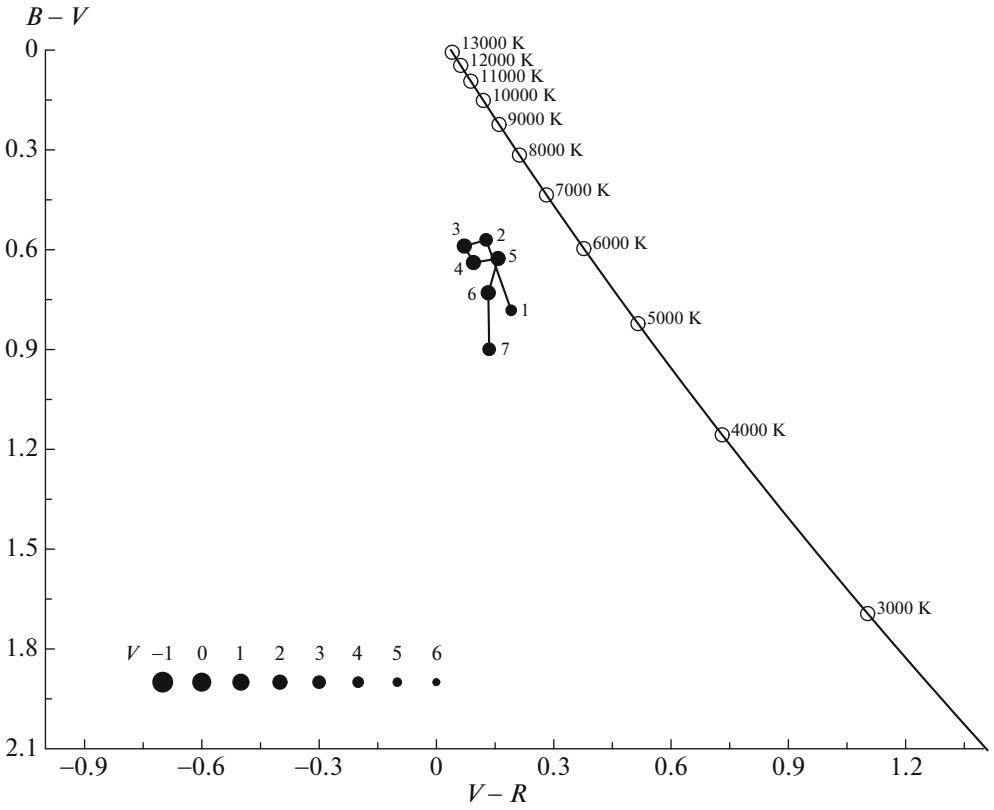

Fig. 7. Two-color diagram for meteor No. 27 (SPO).

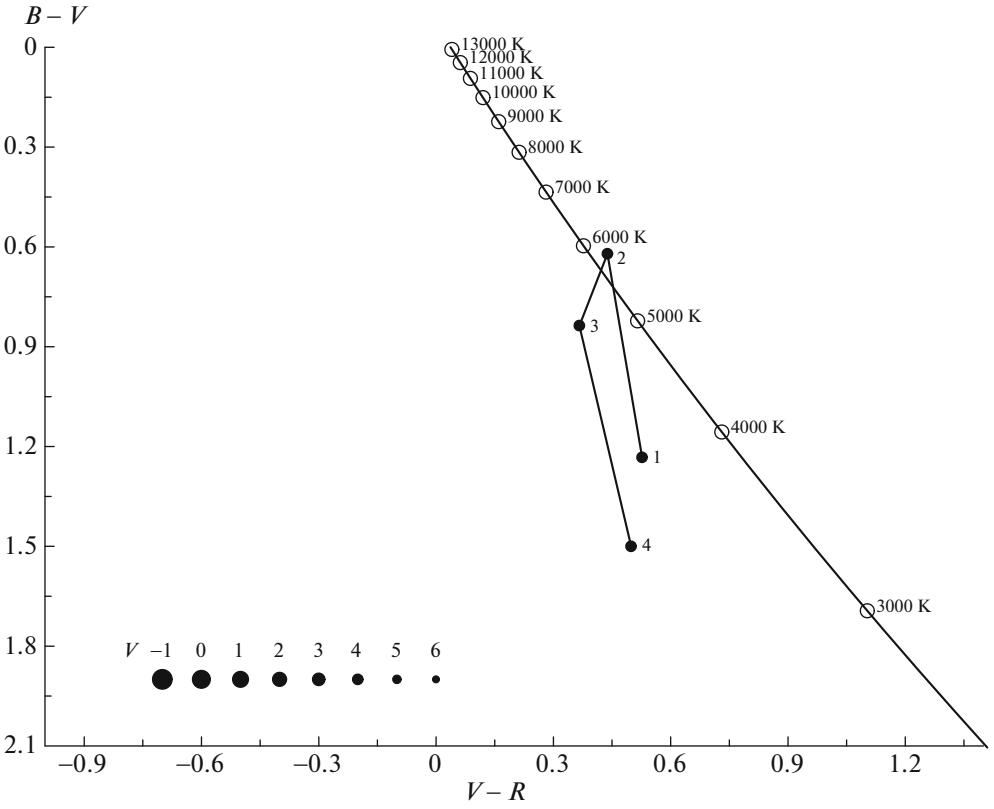

Fig. 8. Two-color diagram for meteor No. 37 (SPO).

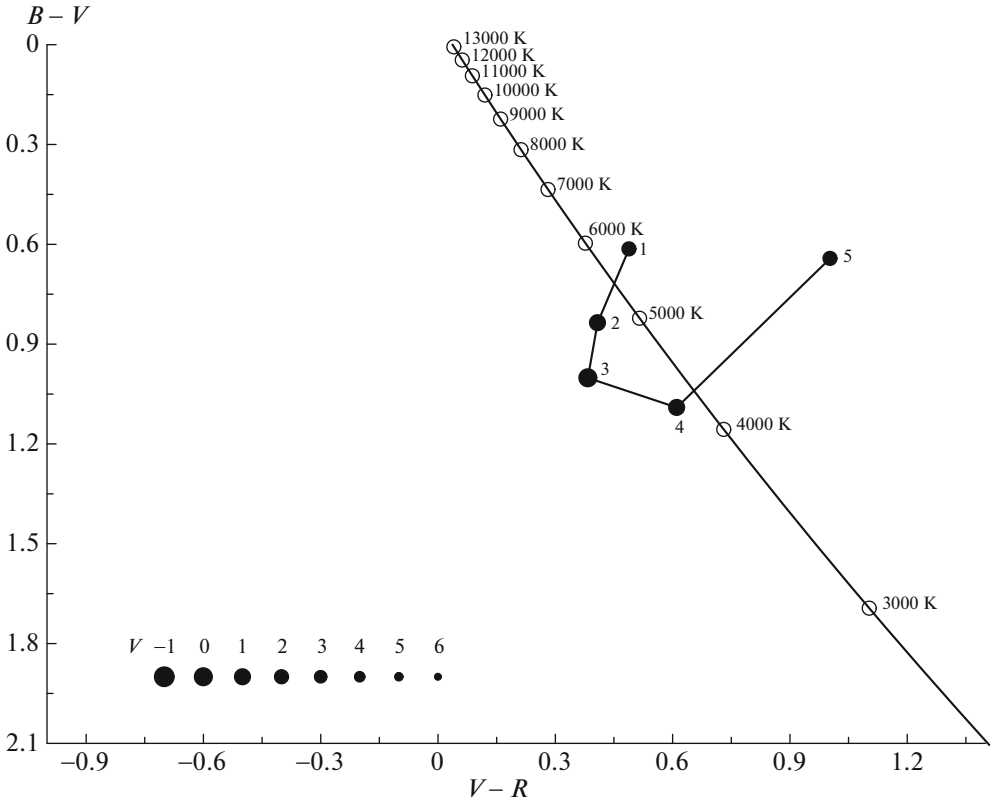

Fig. 9. Two-color diagram for meteor No. 14 (SPO).

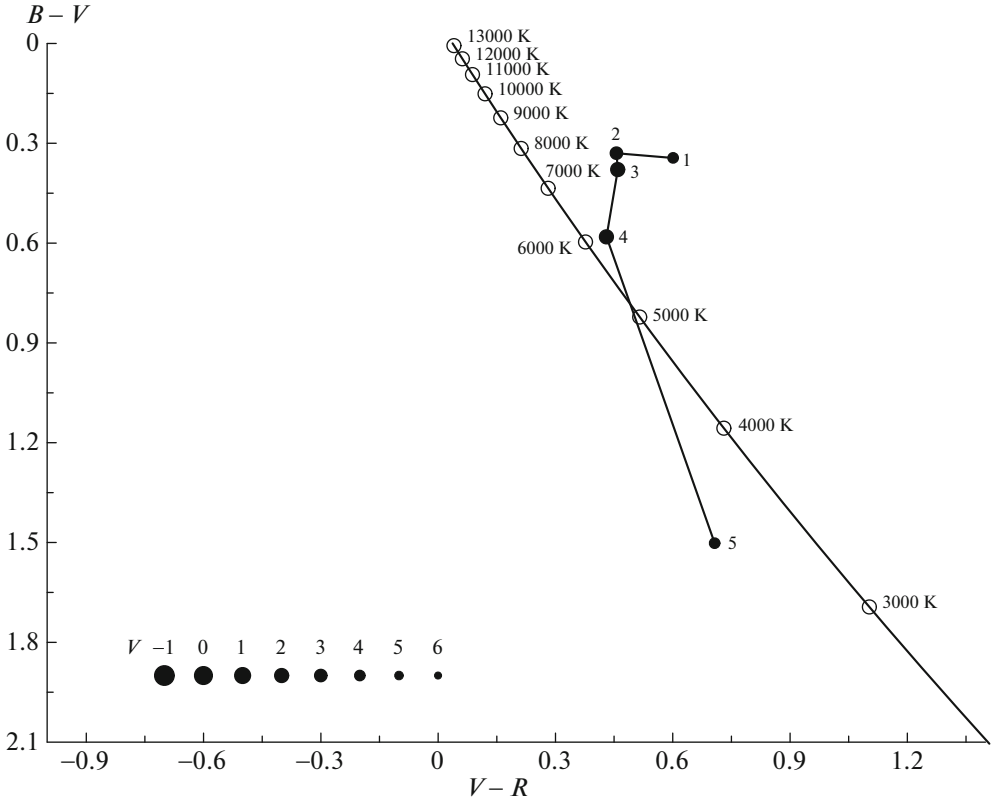

Fig. 10. Two-color diagram for meteor No. 6 (SPO).

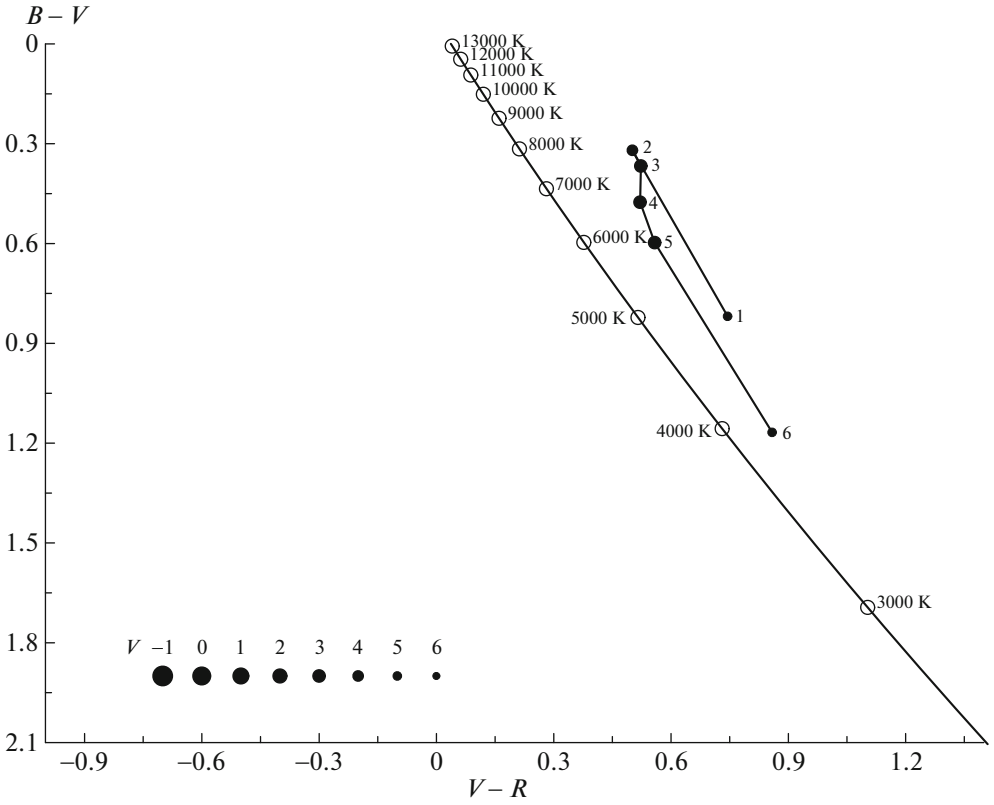

Fig. 11. Two-color diagram for meteor No. 3 (SPO).

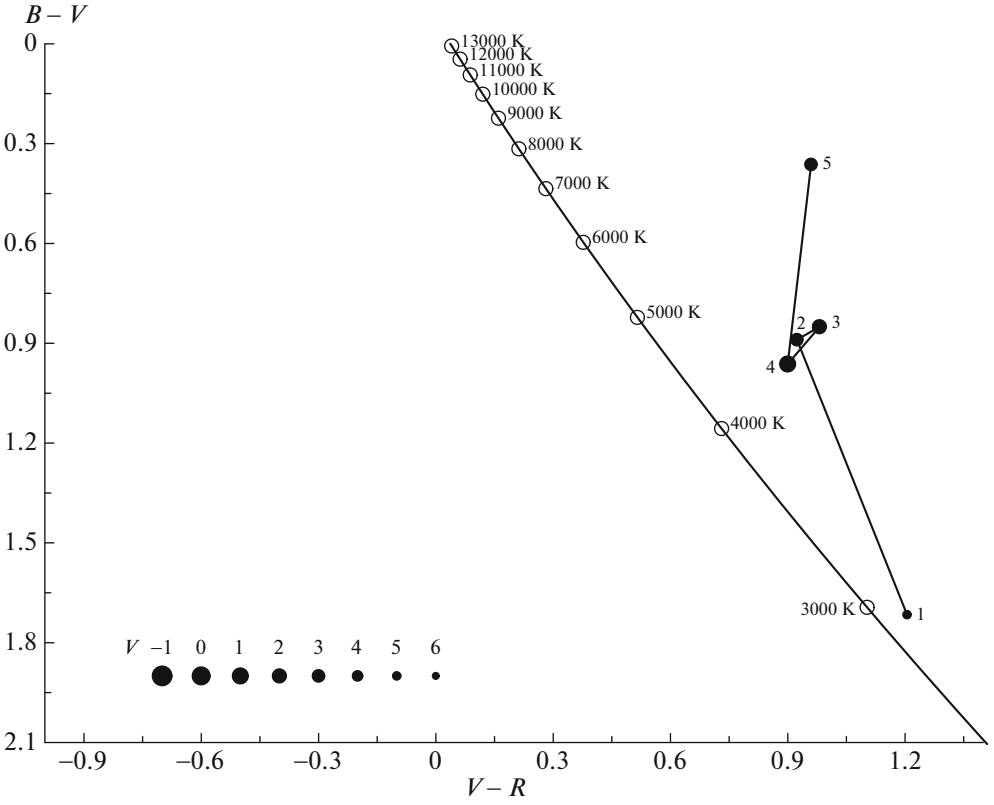

Fig. 12. Two-color diagram for meteor No. 21 (SPO).

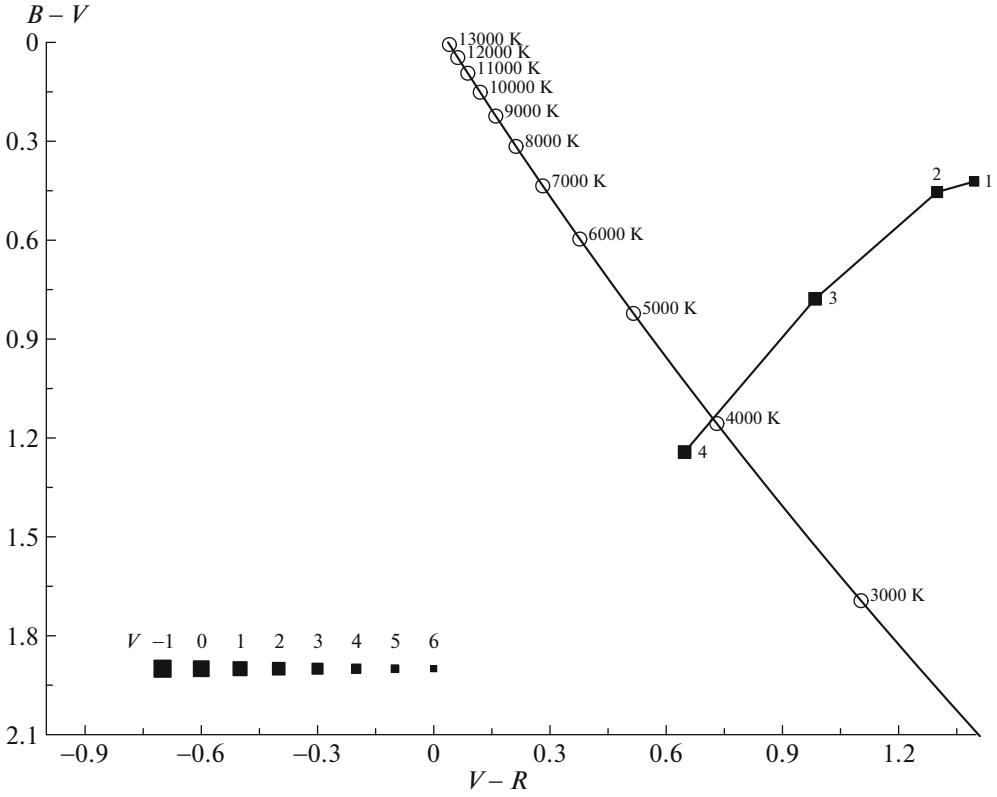

Fig. 13. Two-color diagram for meteor No. 23 (PER).

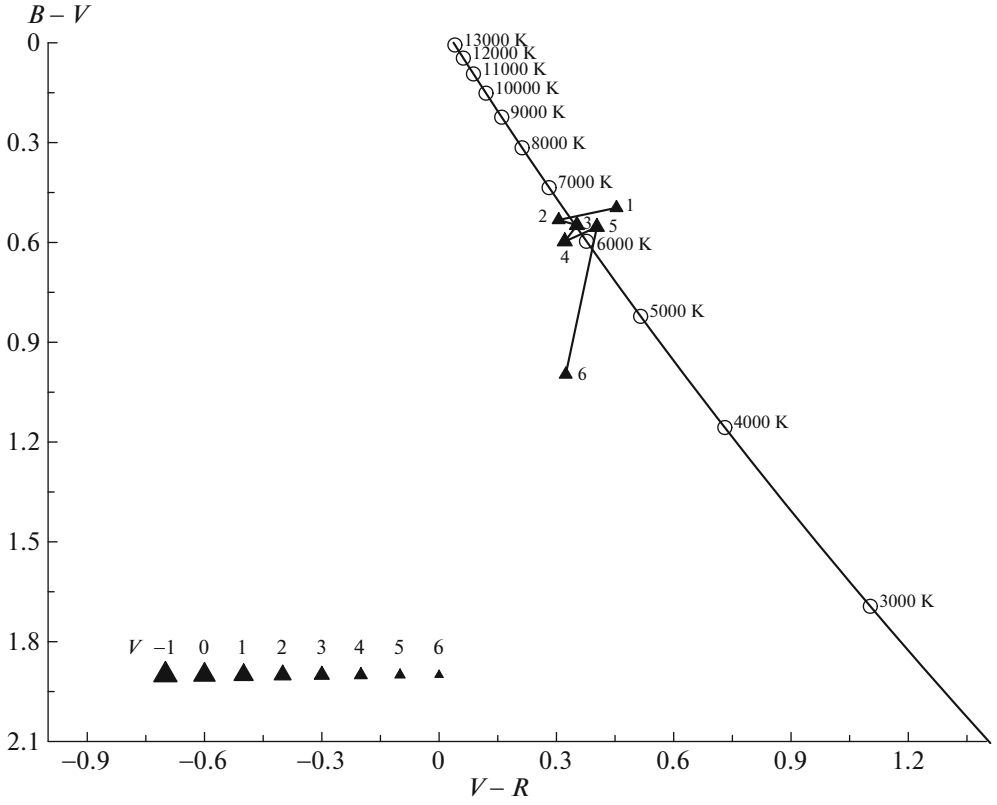

Fig. 14. Two-color diagram for meteor No. 33 (STA).

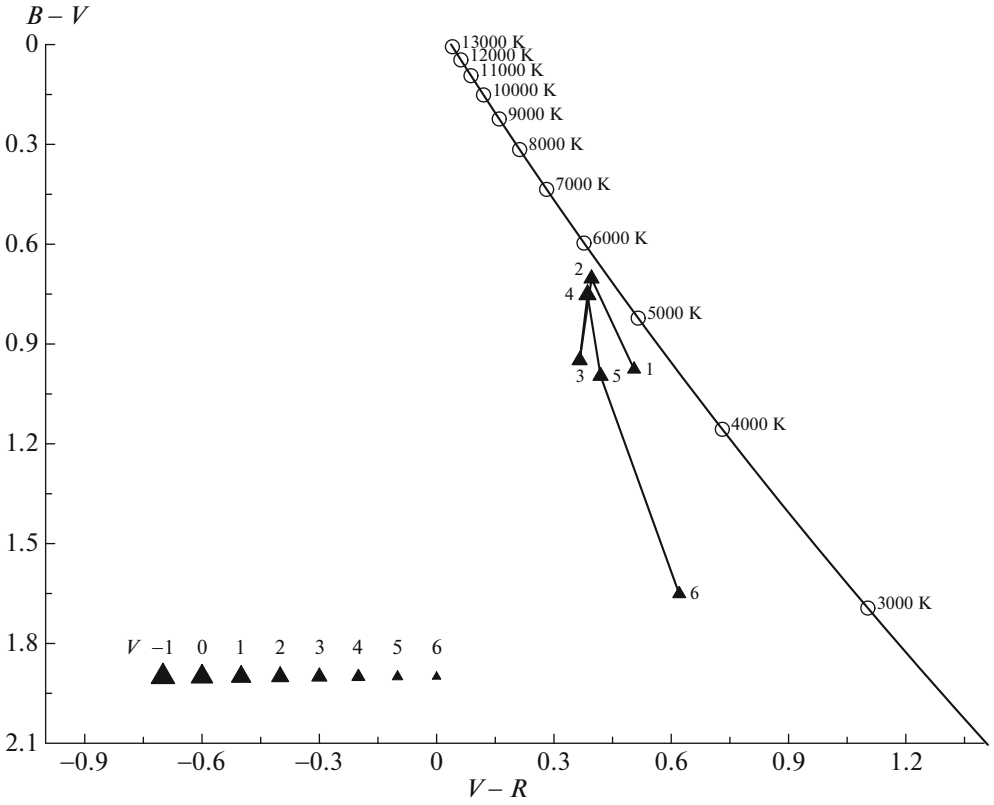

Fig. 15. Two-color diagram for meteor No. 40 (NTA).

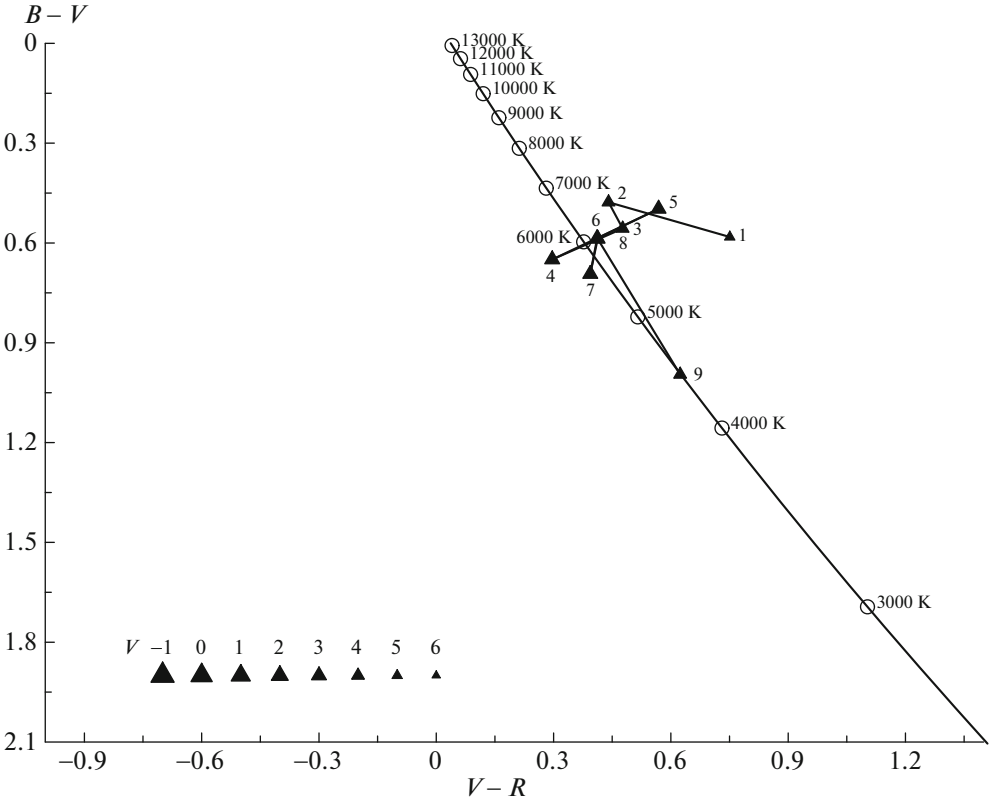

Fig. 16. Two-color diagram for meteor No. 41 (STA).

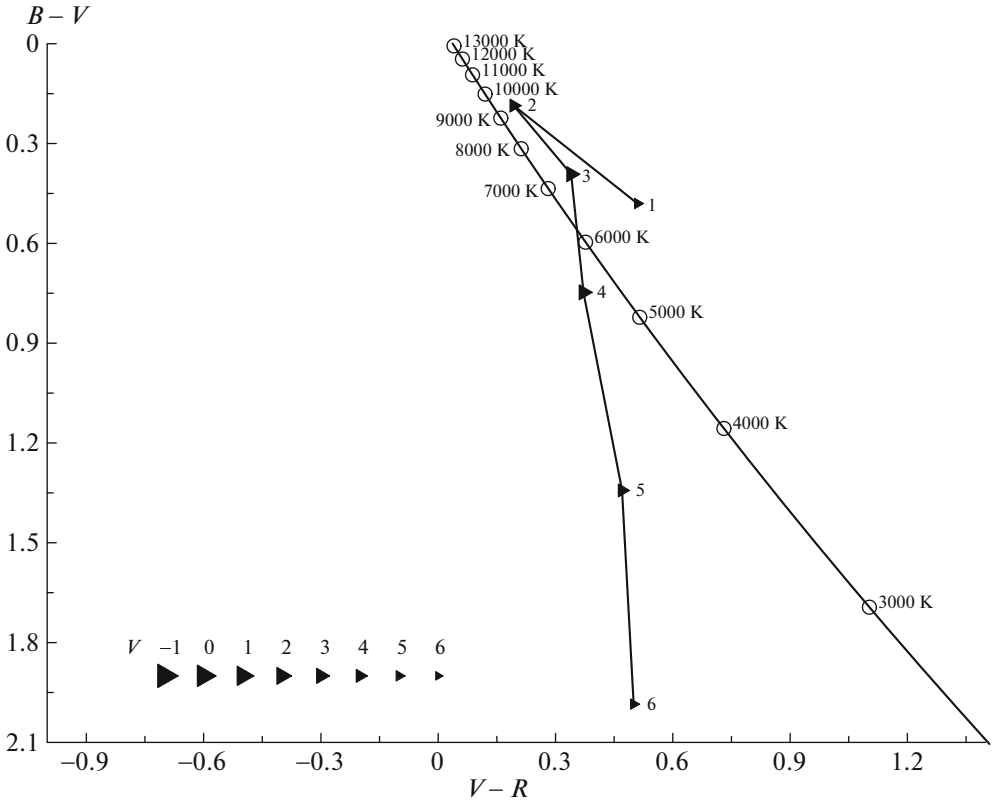

Fig. 17. Two-color diagram for meteor No. 49 (GEM).

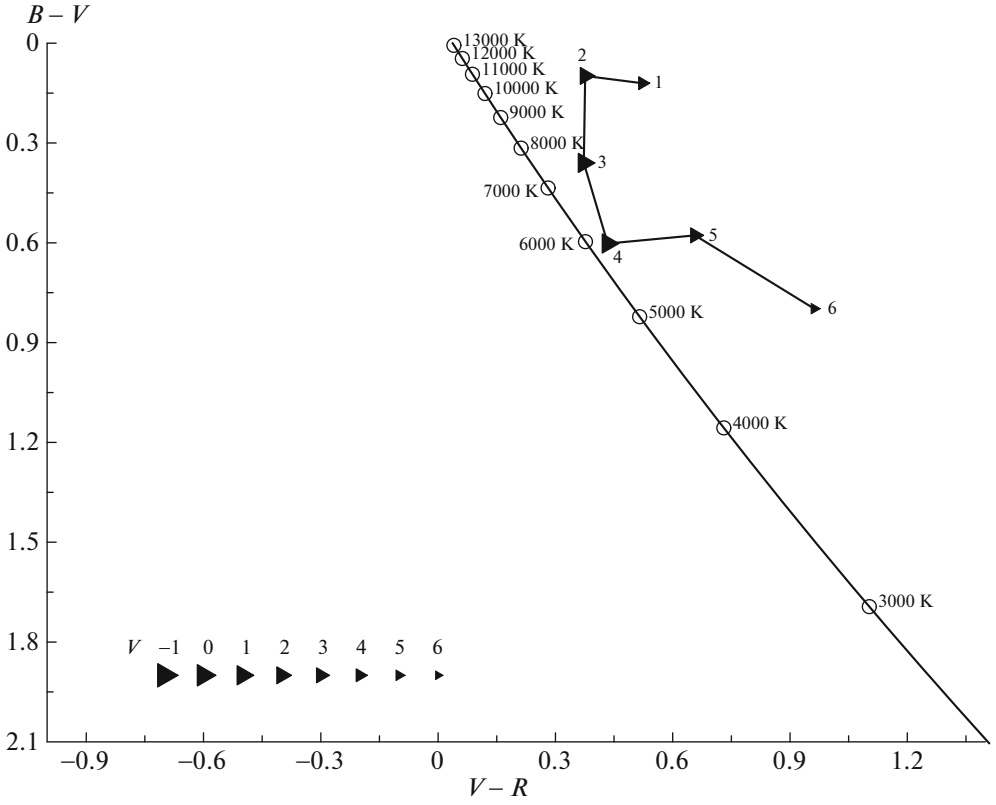

Fig. 18. Two-color diagram for meteor No. 53 (GEM).

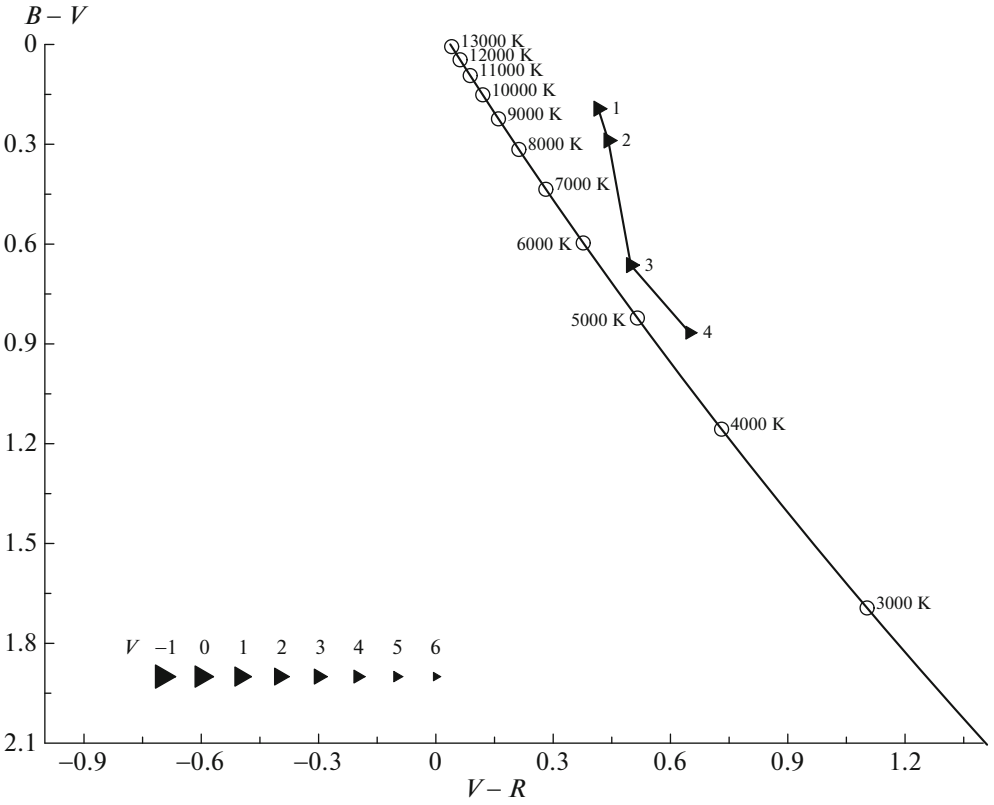

Fig. 19. Two-color diagram for meteor No. 45 (GEM).

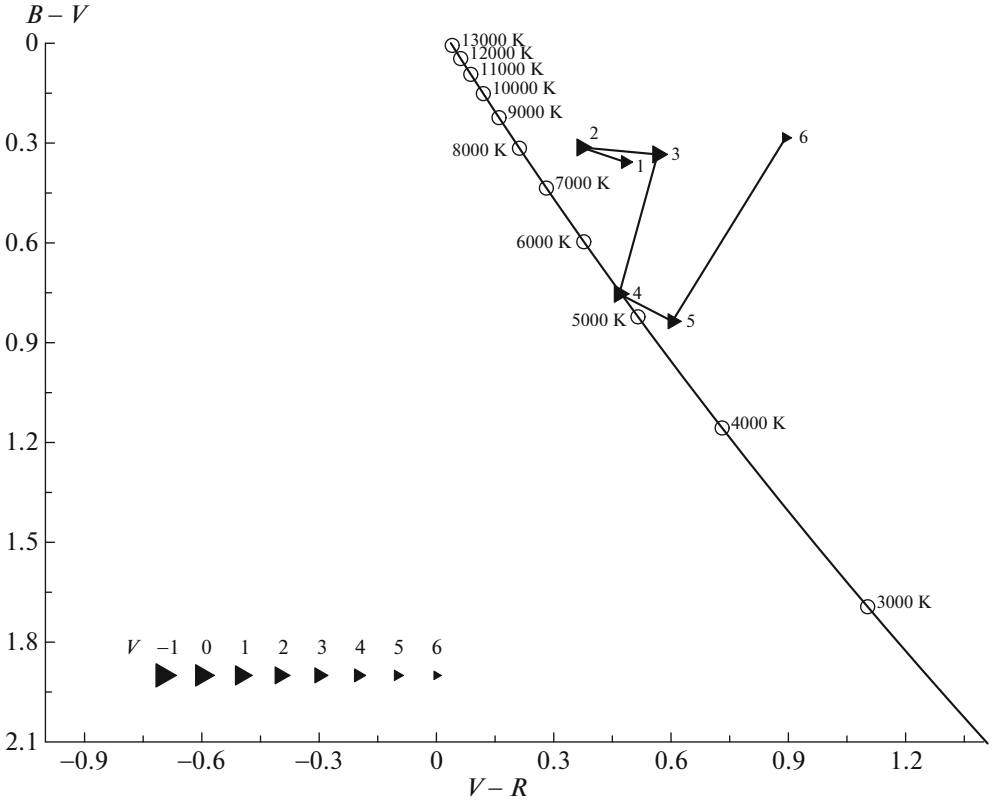

Fig. 20. Two-color diagram for meteor No. 57 (GEM).

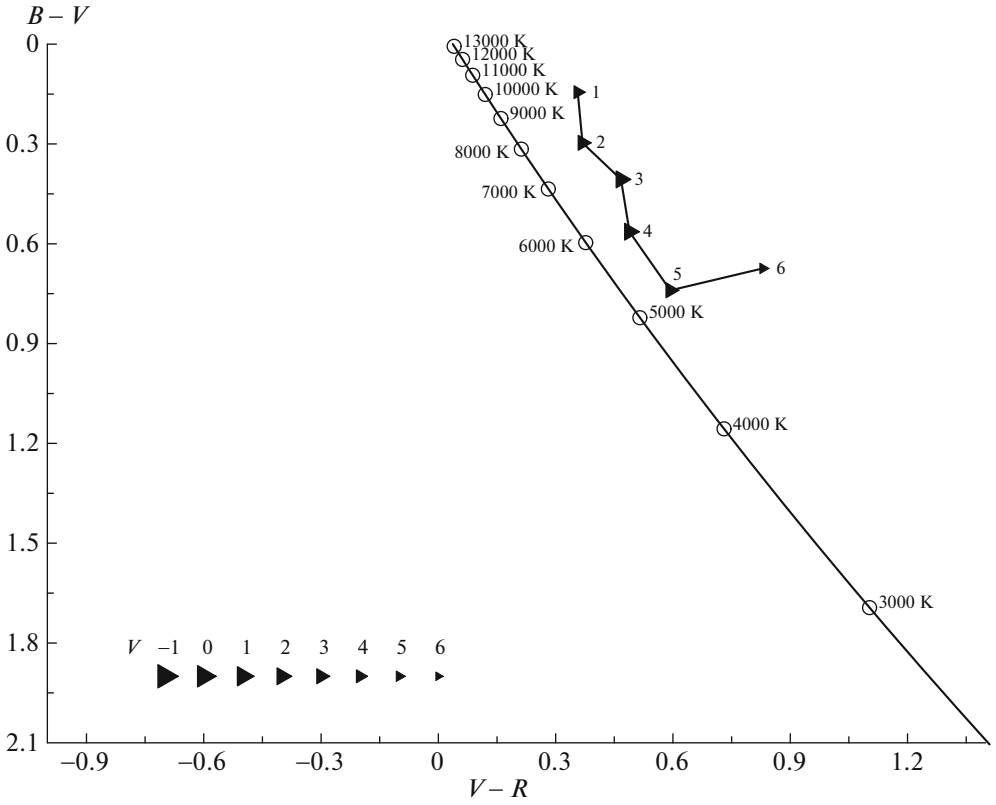

Fig. 21. Two-color diagram for meteor No. 48 (GEM).

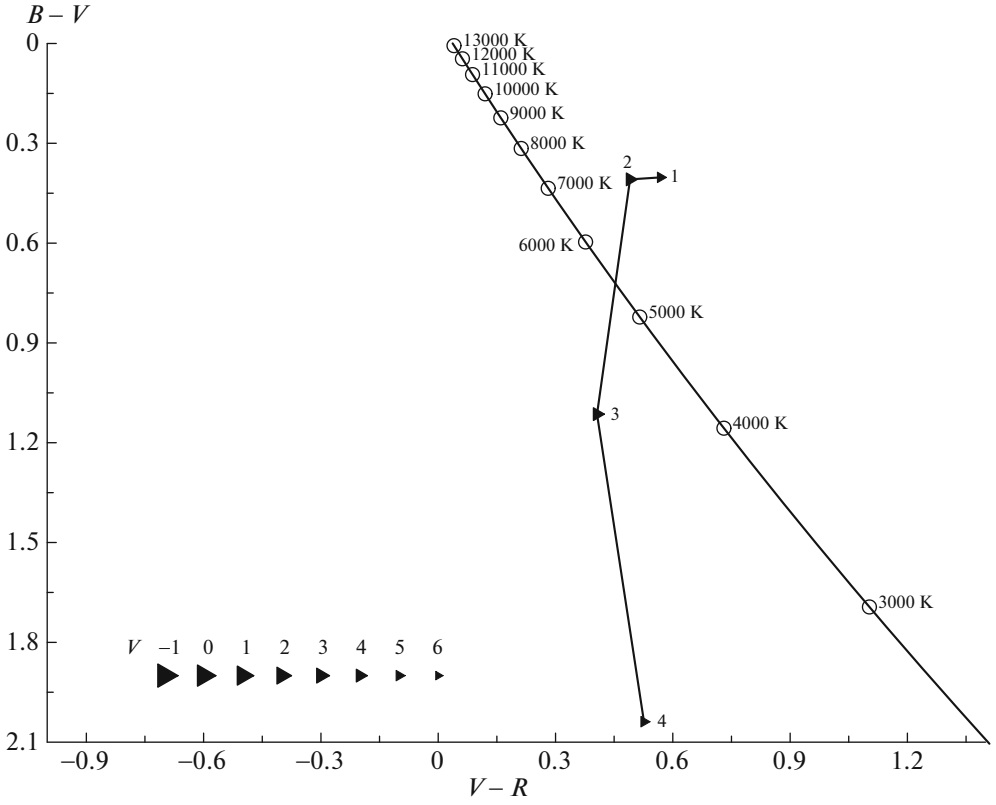

Fig. 22. Two-color diagram for meteor No. 43 (GEM).

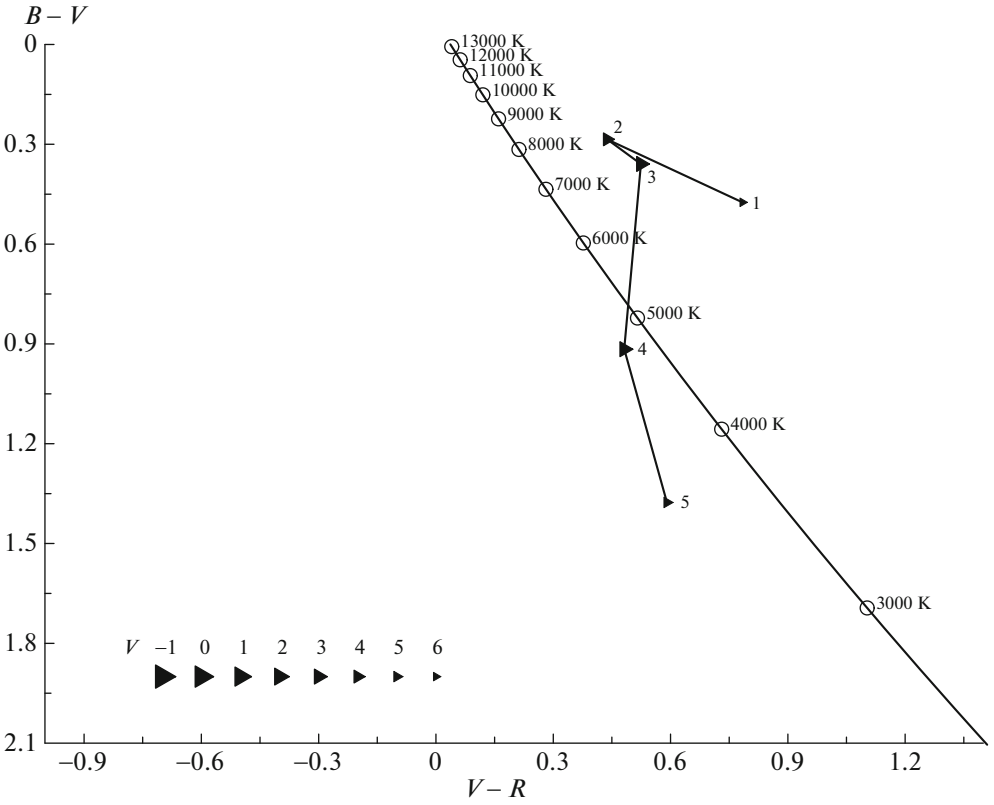

Fig. 23. Two-color diagram for meteor No. 50 (GEM).

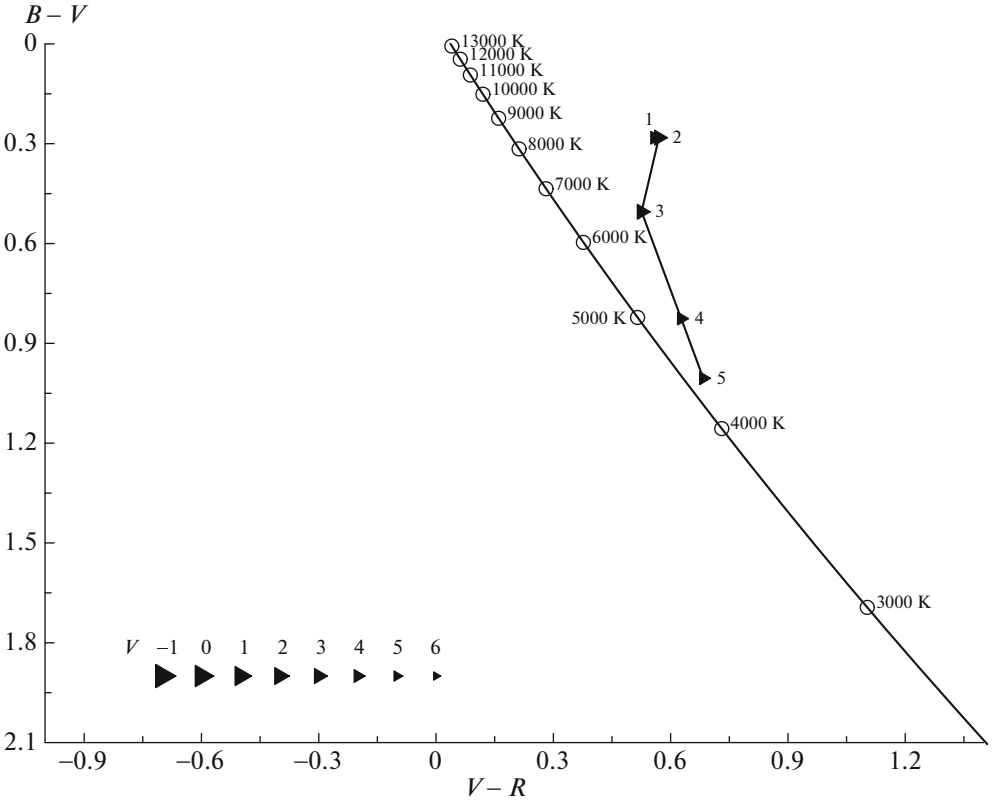

Fig. 24. Two-color diagram for meteor No. 61 (GEM).

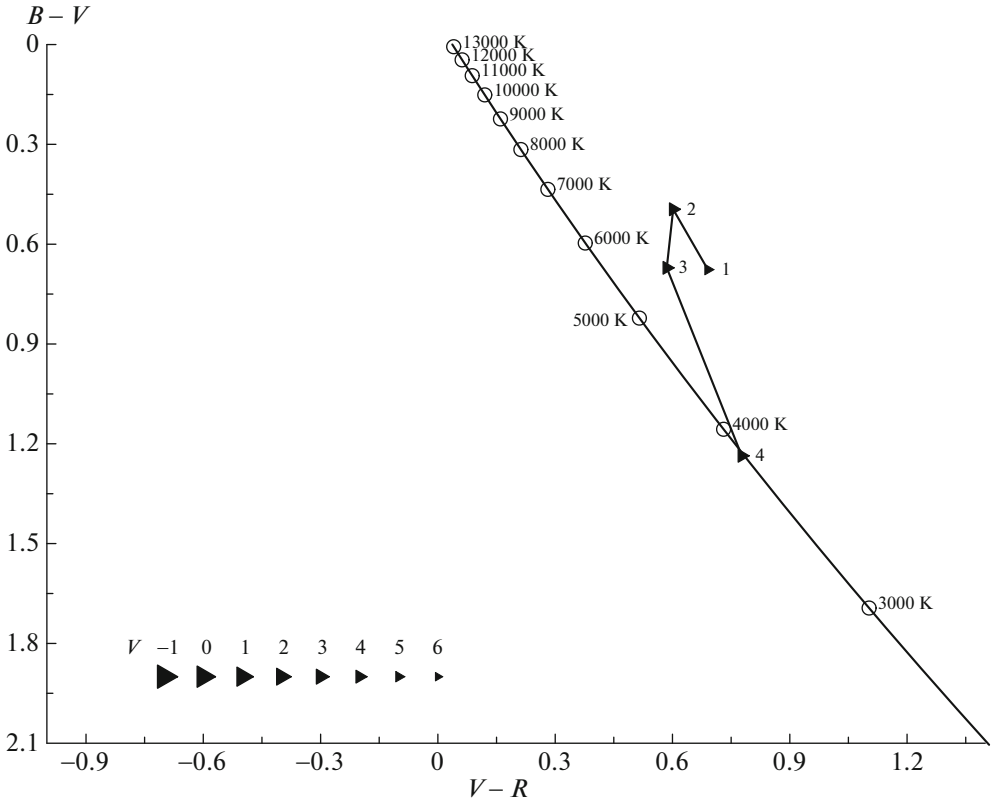

Fig. 25. Two-color diagram for meteor No. 58 (GEM).

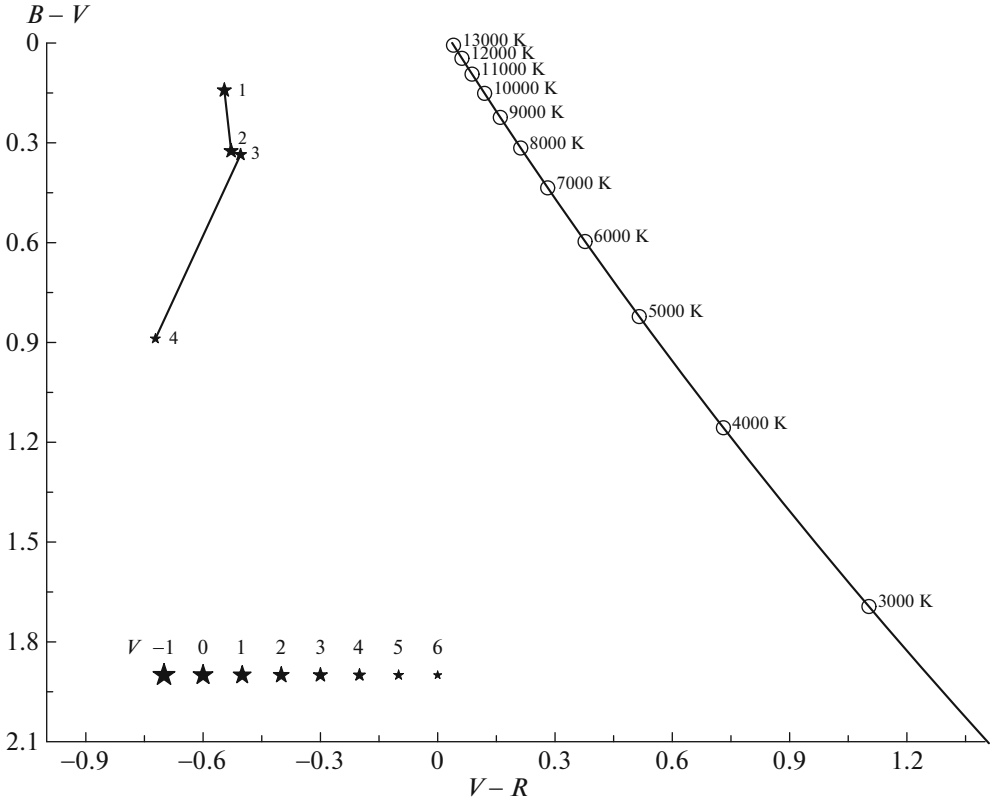

Fig. 26. Two-color diagram for meteor No. 66 (LYR).

two-color diagrams. Comparison with the Na–Mg–Fe ternary diagram shows that the color classification of meteors does not repeat the modern spectral classification.

Nevertheless, the specific form of the dependence of the colors on the dynamical characteristics of a shower remains unclear. It is planned to carry out additional studies, in order to better understand the character of this dependence. BVR observations of the same and other major and minor meteor showers whose mean orbits are known may help elucidate which dynamical parameters of the showers yield similar colors, and which bring about color differences. Conducting double-station observations (on the MMT-9 are now in an experimental regime) simultaneously with BVR observations should help determine the orbital elements of sporadic meteors, enabling studies of which elements unify meteors in a given shower with sporadic meteors located in the same region of the two-color diagram. Calculation of synthetic color indices using spectra of meteors known from the literature will enable comparisons of the color and spectral classifications, and identification of emission lines of various elements that make the largest contributioin to the visible colors.

ACKNOWLEDGMENTS

We thank G.M. Beskin, S.V. Karpov (Special Astrophysical Observatory of the Russian Academy of Sciences, Kazan (Volga Region) Federal University [KFU]), A.V. Biryukov (Sternberg Astronomical Institute, KFU), S.F. Bondar'†, E.A. Ivanov, E.V. Katkova, N.V. Orekhova, A.V. Perkov (Arkhyz Optical Observation Station of the Research and Production Corporation "Precision Systems and Instruments"), and V.V. Sasyuk (Parallax Company, KFU) for organizing and conducting the observations, the preliminary processing of the data, creating and managing the observational catalog, and useful discussions of our results.

FUNDING

This work was partially funded by the subsidy 3.6714.2017/8.9 allocated to Kazan Federal University for the state assignment in the sphere of scientific activities. The work is partially performed according to the Russian Government Program of Competitive Growth of Kazan Federal University and the Russian Foundation for Basic Research, grant no. 18-32-00895 mol_a.

†Deceased.

REFERENCES

1. E. Sansom, J. Ridgewell, P. Bland, and J. Paxman, in *Proceedings of the International Meteor Conference, Egmond, the Netherlands, 2016,* Ed. by A. Roggemans and P. Roggemans (2016), p. 267.
2. M. Beech, Quart. J. R. Astron. Soc. **28**, 445 (1987).
3. G. Wu and Z. Zhang, Chin. Astron. Astrophys. **27**, 435 (2003).
4. A. McBeath, WGN, J. IMO **18**, 114 (1990).
5. A. McBeath, WGN, J. IMO **19**, 198 (1991).
6. G. Zay, WGN, J. IMO **21**, 268 (1993).
7. A. Olech and P. Woźniak, Earth, Moon Planets **73**, 157 (1996).
8. L. G. Jacchia, Astron. J. **62**, 358 (1957).
9. Z. Ceplecha, Bull. Astron. Inst. Czechosl. **10**, 39 (1959).
10. J. Davis, Smith. Contr. Astroph. **7**, 233 (1963).
11. J. Davis, Mon. Not. R. Astron. Soc. **126**, 445 (1963).
12. L. Kohoutek, Bull. Astron. Inst. Czechosl. **14**, 172 (1963).
13. Z. Ceplecha, J. Grygar, and L. Kohoutek, Bull. Astron. Inst. Czechosl. **16**, 123 (1965).
14. M. Hajduková, Bull. Astron. Inst. Czechosl. **18**, 187 (1967).
15. M. Hajduková, Bull. Astron. Inst. Czechosl. **23**, 350 (1972).
16. M. Hajduková, Bull. Astron. Inst. Czechosl. **24**, 229 (1973).
17. J. Štohl and M. Hajduková, Bull. Astron. Inst. Czechosl. **30**, 13 (1979).
18. U. Sperberg, WGN, J. IMO **18**, 111 (1990).
19. F. Ocaña, J. Zamorano, and J. Gallego, in *Proceedings of the International Meteor Conference, Sibiu, Romania, 2011,* Ed. by M. Gyssens and P. Roggemans (2012), p. 48.
20. M. Hajduková, Bull. Astron. Inst. Czechosl. **25**, 365 (1974).
21. P. M. Millman, Ann. Harvard College Observ. **82**, 149 (1935).
22. P. M. Millman, Smith. Contr. Astrophys. **7**, 119 (1963).
23. J. Borovička, Planet. Space Sci. **42**, 145 (1994).
24. J. Borovička, P. Koten, P. Spurný, J. Boček, and R. Štork, Icarus **174**, 15 (2005).
25. P. M. Millman, Ann. Harvard College Observ. **82**, 113 (1932).
26. J. Borovička, in *Proceedings of the International Meteor Conference, Egmond, the Netherlands, 2016,* Ed. by A. Roggemans and P. Roggemans (2016), p. 34.
27. V. Vojáček, J. Borovička, P. Koten, P. Spurný, and R. Štork, in *Proceedings of the International Meteor Conference, Egmond, the Netherlands, 2016,* Ed. by A. Roggemans and P. Roggemans (2016), p. 333.
28. A. Drouard, P. Vernazza, S. Loehle, J. Gattacceca, et al., Astron. Astrophys. **613**, A54 (2018).
29. H. L. Johnson and W. W. Morgan, Astrophys. J. **117**, 313 (1953).

30. I. Groeneveld and G. P. Kuiper, Astrophys. J. **120**, 529 (1954).
31. J. K. Davies, D. J. Tholen, and D. R. Ballantyne, ASP Conf. Ser. **107**, 97 (1996).
32. J. Luu and D. Jewitt, Astron. J. **112**, 2310 (1996).
33. D. Jewitt, Astron. J. **150**, 201 (2015).
34. T. Cardona, P. Seitzer, A. Rossi, F. Piergentili, and F. Santoni, Adv. Space Res. **58**, 514 (2016).
35. W. Park, S. Pak, H. Shim, H. A. N. Le, M. Im, S. Chang, and J. Yu, Adv. Space Res. **57**, 509 (2016).
36. A. Biryukov, G. Beskin, S. Karpov, S. Bondar, E. Ivanov, E. Katkova, A. Perkov, and V. Sasyuk, Baltic Astron. **24**, 100 (2015).
37. M. S. Bessell, Publ. Astron. Soc. Pacif. **102**, 1181 (1990).
38. A. Zakharov, A. Mironov, A. Biryukov, N. Kroussanova, et al., Acta Astron. **65**, 197 (2015).
39. S. Karpov, G. Beskin, A. Biryukov, S. Bondar, E. Ivanov, E. Katkova, A. Perkov, and V. Sasyuk, Rev. Mex. Astron. Astrof., Ser. Conf. **48**, 91 (2016).
40. S. Karpov, N. Orekhova, G. Beskin, A. Biryukov, et al., Rev. Mex. Astron. Astrof., Ser. Conf. **48**, 97 (2016).
41. Z. Ceplecha, Bull. Astron. Inst. Czechosl. **8**, 51 (1957).
42. F. L. Whipple and L. G. Jacchia, Smith. Contr. Astrophys. **1**, 183 (1957).
43. D. E. B. Fleming, R. L. Hawkes, and J. Jones, in *Meteoroids and Their Parent Bodies,* Ed. by J. Štohl and I. P. Williams (1993), p. 261.
44. V. A. Leonov, Solar Syst. Res. **44**, 122 (2010).
45. P. Jenniskens, Q. Nénon, J. Albers, P. S. Gural, et al., Icarus **266**, 331 (2016).
46. J. D. Giorgini, D. K. Yeomans, A. B. Chamberlin, P. W. Chodas, et al., Bull. Am. Astron. Soc. **28**, 1158 (1996).
47. C. Tubiana, C. Snodgrass, R. Michelsen, H. Haack, H. Böhnhardt, A. Fitzsimmons, and I. P. Williams, Astron. Astrophys. **584**, A97 (2015).
48. D. Jewitt and J. Li, Astron. J. **140**, 1519 (2010).
49. G. O. Ryabova, in *Proceedings of the European Planetary Science Congress, 2008* (2008), id. A-00226.
50. C. Rodrigo, A. Bayo, E. Solano, and D. Barrado y Navascués, ASP Conf. Ser. **485**, 321 (2014).
51. M. S. Bessell, F. Castelli, and B. Plez, Astron. Astrophys. **333**, 231 (1998).
52. I. Halliday, Astrophys. J. **131**, 25 (1960).

Translated by D. Gabuzda